

360 kA Hall-Héroult Cell Retrofit Using Inert Anodes and Stable Cathodes

Louis Bugnion¹, René von Kaenel², Laure von Kaenel³

1. Project Manager

2. CEO

3. Junior Project Manager

KAN-NAK SA, 3960 Sierre, Switzerland

Louis.Bugnion@kannak.ch

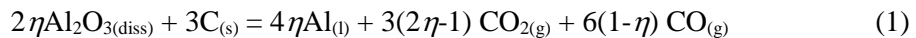
Abstract

Experiments more than one decade ago demonstrated the feasibility of operating a Hall-Héroult cell with metallic anodes at 25 kA. In March 2019, ELYSIS confirmed the existence of stable anodes and cathodes during the TMS annual meeting in San Antonio. It was often claimed that the reduction of alumina demands one extra volt per cell when operating with Inert Anodes, which represents about 3 kWh/kg Al in addition to the amount currently required by the traditional Hall-Héroult process. This paper gives a potential solution to achieve a specific energy consumption comparable to the best in class Hall-Héroult cells using metallic inert anodes and cathodes. The engineered solution is for the retrofit of a typical 360 kA cell.

Keywords: Inert anode, inert cathode, specific energy consumption in aluminium reduction cells, cell retrofit, Hall-Héroult process.

1. Introduction

Since the early days of aluminium smelting, the dream of operating a Hall-Héroult cell producing oxygen as a by-product rather than carbon dioxide has been pursued. The fundamental difference between both solutions comes from the reduction of the alumina. Traditionally, the oxygen burns the anode leading to the well-known chemical equilibrium [1]:



where:

η Current efficiency, fraction.

The use of a so-called inert anode allows realizing a direct reduction of the alumina by equation (2), avoiding both carbon monoxide and carbon dioxide emissions [2]. In this paper, we shall use the term “inert anode” even if it is not strictly inert and may need to be replaced every few months or years.



The challenge when using an inert anode is to design a cell operating at low specific energy consumption at the right thermal equilibrium. In thermal equilibrium the net heat generated in the cell and connecting busbars is equal to the heat loss. Considering the enthalpy (heating and formation) of reaction (1) at 960 °C [3] and the Faraday equation, the net heat generation for the carbon anode Hall-Héroult cell is equal to:

$$Q_{HH} = [V_{cell} - (1.6493\eta + 0.48032)]I \quad (3)$$

where:

Q_{HH} Hall-Héroult cell total heat generated, kW

V_{Cell} Cell voltage, V

I Cell current, kA

By considering the enthalpy of reaction (2), it is easy to show that the inert anode process leads to the net heat generation:

$$Q_{IA} = (V_{Cell} - 3.108\eta)I \quad (4)$$

where:

Q_{IA} Inert anode cell heat generation, kW.

The last two terms in equation (3) in round bracket and the last term in equation (4) represent the equivalent voltage to make aluminium, derived from the enthalpy of reactions (1) and (2), respectively, which is subtracted since the reactions are endothermic. In the inert anode cell, the voltage to make aluminium is obviously much higher (2.953 V at 95 % current efficiency) than in the carbon anode cell (2.047 V at 95 % current efficiency), and this is because burning carbon is exothermic and gives energy back to the process. The difference is 0.91 V or 2.85 kWh/kg Al.

Therefore, the net heat generation in the inert anode cell is much lower for the same current and voltage drop. This is to say that also heat loss from the inert anode cell must be much lower. In order to quantify the difference between both technologies, let us consider a 360 kA cell operated at 4.15 V with 95 % current efficiency. This means a specific energy consumption of 13.02 kWh/kg Al, which can be qualified as best-in-class. The Hall-Héroult cell operates with 757 kW net heat generation and loss, while the inert anode technology must operate with 431 kW net heat generation and loss to achieve the same voltage drop and, consequently, comparable specific energy consumption. The challenge is how to keep the heat loss of the inert anode cell so low and keep the desired bath temperature, mentioned below.

We believe that it is possible to operate both technologies with comparable voltage drops, current and current efficiencies while keeping the aforementioned difference in heat loss. Reference [4] presented potential concepts to achieve such a task. More than a decade ago, operation with metallic anodes in a 25 kA cell [5] confirmed the possibility to produce primary aluminium with inert anodes and gave a basic understanding for retrofitting cells. The announcement of the availability of stable anodes and cathodes during the TMS conference 2019 in San Antonio by ELYSIS gave us the motivation to study the retrofit of a 360 kA cell satisfying the low heat loss constraint while operating with the same specific energy consumption, current and current efficiency.

1.1. Economical Constraints for the Retrofit

Let us first define a number of constraints giving an economical sense to the retrofit solution. The retrofitted cell will consider the following:

- Same line current: 360 kA;
- Same current efficiency: 95 %;
- Minor changes to the existing busbars (flexes to main busbars, shortcuts between busbars);
- Potshell kept as existing, however, shorten by 50 % in length (cut and weld);
- Superstructure kept as existing, however, modified feeders;
- Solid crust above liquid bath covered with pure alumina (held by a structure);
- Low temperature bath chemistry:

CaF ₂	6.0 %
Al ₂ O ₃	4.2 %

LiF	4.5 %
MgF ₂	0.5 %
AlF ₃	11.4 %
KF	5.0 %;

- Liquidus temperature: 893 °C;
- Bath electrical conductivity: 206 Ω⁻¹·m⁻¹.

Under such conditions, the power system including the rectifiers is not impacted. The production remains the same so that the global plant logistic is not affected. Only cells need some investments and the implementation can be performed according to the pot relining schedule, with minimal impact on potroom operations.

1.2. How Can We Achieve Low Heat Loss for the Inert Anode Cell?

The concept shown in Figure 1 [4] consists in increasing the active surface inside the bath. This leads to a smaller cell with much lower shell surface and hence lower heat loss.

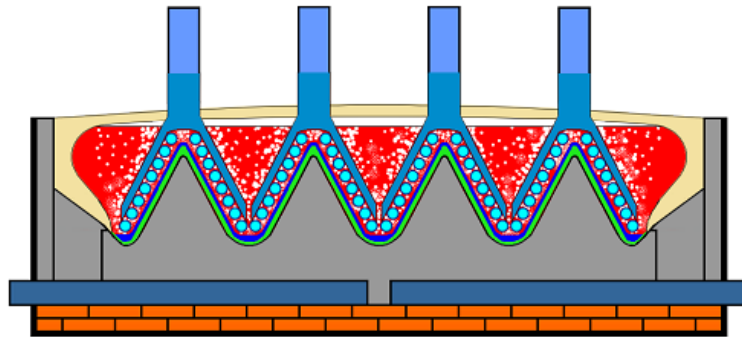


Figure 1. Inert anode and cathode cell concept [3]. The tilted anodes (blue and light blue), oxygen bubbles (white), drained cathode (grey) with wettable surface (green) are represented.

The availability of inert anodes and stable cathodes allow for a new path of the current inside the cell. In this modeling work, the anode is made of NILO (nickel-iron alloy) casted in any shape. Reference [6] gives more details concerning NILO material. As an example, Figure 2 shows a NILO casted anode used in year 2005 in the 25 kA MOLTECH cell.



Figure 2. Example of NILO anode tested in a 25 kA cell [4].

Titanium diboride (TiB₂) plates act as the cathode and lead the current to the liquid metal. Ceramic supports hold the cathodes in the metal and bath. Such ceramic structure and titanium diboride

plates were used in 1982 at the Alusuisse R&D center in Chippis to obtain a constant and low anode-cathode distance (ACD) in a so called “low energy cell”. A 6° angle of the anodes and cathodes against verticality (see Figure 4) allows for cell voltage drop adjustment and improved oxygen flow. When moving the beam by 10 mm, the ACD changes by 1 mm.

In this geometry, the cathode is inside the liquid bath. The aluminium wets the titanium diboride plates and flows to the bottom of the cell in the liquid aluminium pool. The current flows from the TiB_2 cathodes into the liquid metal, then to thin carbon blocks and finally to the collector bars. The bottom carbon blocks are no longer the cathode except for a very small amount of current flowing directly from the anodes to the liquid metal. The collector bars are made of copper using a so-called RuCTM (Ready to Use Cathode) design, which avoids the rodding process, leads to very low voltage drop and allows for copper recycling.

The anode rod leading the current from the beam to the NILO anode is made of copper, which is able to adequately resist an environment consisting in a mixture of oxygen and fluoride gases.

The implementation of said design constraints in a three-dimensional model of a well-known 360 kA technology led to the following cell geometry (Figure 3). In the spirit of a retrofit, the busbars geometry has been modified as little as possible, but it is evident that some optimization is possible. The inert anode cell is shorter as only 20 over 40 anode clamps are used. This is to reduce the shell surface and, as a direct consequence, pot heat loss.

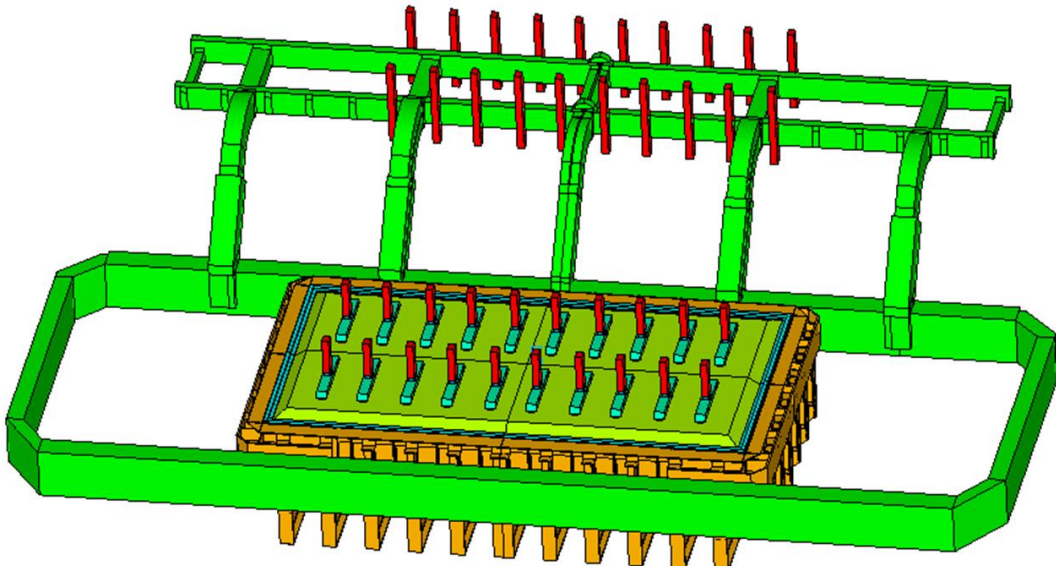


Figure 3. Model of the 360 kA Inert Anode cell (busbars have been anonymized).

Figure 4 shows the details of the anodes and cathodes. The grid structure of the anodes allows feeding alumina from the top. The very high volume of bath and global bath velocity give much more time for the alumina dissolution process than in a conventional Hall-Héroult cell. The volume of liquid bath in the inert anode cell is close to 30 liters per kA or more than 2.5 times greater than what is commonly found on its traditional counterparts. Finally, said anode grid arrangement is also useful for the oxygen release and bath movement.

The inert anode current density is 0.97 A/cm² (with the total anode projected surface as active surface) while the Hall-Héroult cell operates with an anode current density of 0.89 A/cm². Furthermore, the 25 kA MOLTECH cell demonstrated that the inert anode can be operated with

a current density of 1.40 A/cm^2 . The proposed solution applies for a retrofit, but a green field project has the potential of significantly increasing the cell productivity and further improving KPI's. This, however, is beyond the scope of this paper.

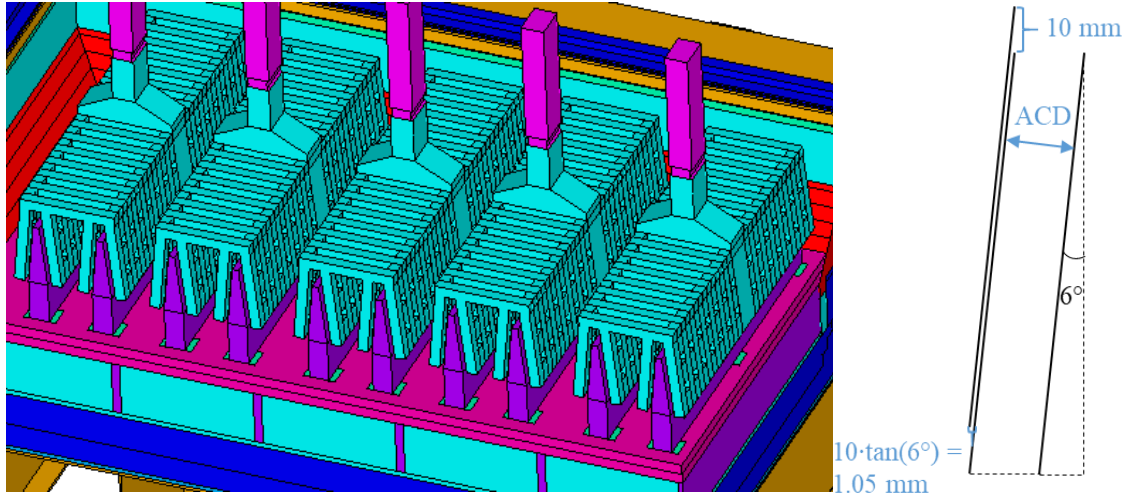


Figure 4. Inert Anodes and Inert Cathodes geometry (left). Sketch illustrating an ACD change of 1 mm caused by a 10 mm displacement of the anode beam (right).

2. Modelling Results

2.1. Energy and Heat Balance of the 360 kA Inert Anode Cell

The inert anode is not consumed and the cathode is solid therefore the anode to cathode distance (ACD) is constant over time and no magneto-hydrodynamic instabilities may take place. This allows operating with a smaller ACD. However, the ACD must be large enough to satisfy both the electrolysis process and the heat production. The side ledge protects the lining and is part of the thermal balance of the cell. The 6° angle of the anode leads the oxygen to the surface avoiding the re-oxidation of the aluminium droplets. The cell internal heat loss is decreased from 647 kW to 314 kW at 360 kA. In order to achieve such a drastic change, the shell is shortened by reducing the number of anode clamps from 40 to 20. The lining, however, is unchanged. Under such modifications, following results are achievable (Table 1).

The inert anode cell voltage breaks down into Ohmic voltage drops ($V_{External}$, V_{Anode} , $V_{Cathode}$, V_{Bath}), the reversible voltage E^{rev} , anodic and cathodic overvoltages η_A and η_C and the bubble voltage V_{bub} .

$$V_{Cell} = V_{External} + V_{Anode} + V_{Cathode} + V_{Bath} + E^{rev} + \eta_A + \eta_C + V_{bub} \quad (5)$$

The reversible voltage obtained from the Gibbs energy differences and the activity of the dissolved alumina [7] is 2.232 V (1.205 V for the Hall-Héroult cell). This is the origin of the claim that the inert anode cell needs one more volt to operate.

The anodic reaction overvoltage of 110 mV reported in [6] for the NILO anode with external coating is assumed. Thanks to the grid structure of the metallic anode, a low bubble voltage is expected and here we assumed that it is zero. Due to the lack of experimental data, the bubble voltage is neglected in (5) for the inert anode cell (assumed to be 111 mV for the Hall-Héroult cell). In case it would be non-negligible, the ACD would be decreased to keep the same cell voltage.

The external voltage drop V_{External} is 329 mV assuming minor modifications on the existing busbars.

Table 1. Hall-Héroult and inert anode cell parameters.

	Unit	Hall-Héroult cell	Inert Anode cell
Amperage	kA	360	360
Gross voltage	V	4.15	4.15
Current efficiency	%	95.0	95.0
Specific energy consumption	kWh/kgAl	13.02	13.02
Production	kgAl/pot day	2755	2755
External voltage (coll. bars to anode bi-metal)	mV	306	329
External resistance	$\mu\Omega$	0.85	0.91
Anode voltage (including anode change, anode effect)	mV	365	224
Anode resistance	$\mu\Omega$	1.02	0.62
Cathode voltage drop (CVD)	mV	257	314
Cathode resistance	$\mu\Omega$	0.71	0.87
Reversible voltage	V	1.205	2.232
Anodic overvoltage	mV	488	110
Cathodic overvoltage	mV	84	91
Bubble voltage	mV	111	0
Anodic current density (geometry)	A/cm ²	0.89	0.97
ACD with bubbles	cm	4.2	2.2
Internal heat generation	kW	647	314

Figure 5 shows the electric potential distribution over the metallic anode; the anode voltage drop is 224 mV (Ohmic power divided by current) that is significantly lower than the anode voltage drop of the Hall-Héroult cell (365 mV).

Figure 6 shows the electric potential distribution from the cathode to the end of the collector bars; the cathode voltage drop (CVD) is 314 mV (Ohmic power divided by current). It takes advantage of the TiB₂ metallic plates, the low carbon cathode height (265 mm) and the RuC collector bar design using only copper inside the cathode. The resistance of one cathode block is decreased from 14.2 to 8.7 $\mu\Omega$ (20 cathode blocks in Hall-Héroult cell with respect to 10 cathode blocks in inert anode cell).

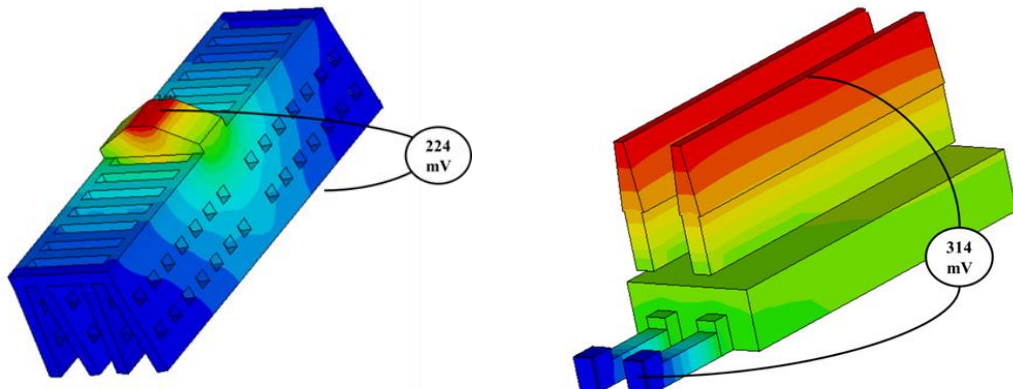


Figure 5. Anode voltage drop.

Figure 6. Cathode voltage drop.

The critical parameter is of course the temperature inside the cell. In our solution, the thermal equilibrium with ledge solidification is achieved for a 22 mm ACD and leads to a maximum bath temperature of 902 °C (9 °C superheat). Figure 7 shows the ledge shape in the bath and metal parts. On the long sides at bath-metal interface, the ledge is approximately 10 cm thick. The cover on top of the cell is made of a 12 cm thick solidified cryolite layer covered with 25 cm pure alumina. A similar layer was used on the experimental 25 kA cell [5] as shown in Figure 8.

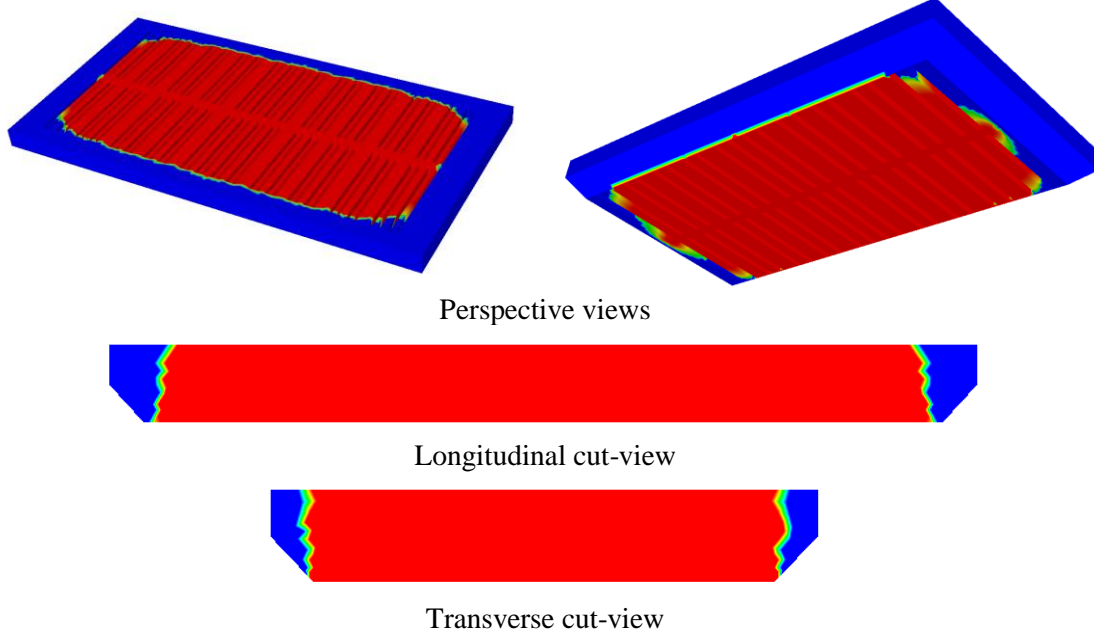


Figure 7. Predicted ledge shape in the bath and metal parts. Solidified cryolite (blue) and liquid bath and metal (red) are represented.

The internal heat loss breakdowns for the Hall-Héroult and inert anode cells are summarized in Table 2. Internal heat loss is decreased by half for the inert anode cell. Heat loss through the anode cover is significantly lower due to thicker cover and pure alumina content. In relative terms, all other heat losses increase, in particular heat loss through the long sides due to higher metal and bath cumulated height.



Figure 8. Alumina top cover on the experimental 25 kA cell.

Table 2. Hall-Héroult and inert anode cell internal heat loss.

Heat losses	kW	%	Heat losses	kW	%
Bottom	38.4	5.9	Bottom	34.5	11.0
Long sides	185.7	28.7	Long sides	109.9	35.0
Short sides	30.0	4.6	Short sides	25.0	7.9
Coll. bars	58.0	9.0	Coll. bars	55.8	17.8
Yokes	106.9	16.5	Yokes	41.8	13.3
Alumina cover	228.0	35.2	Alumina cover	47.0	15.0
Total	647	100.0	Total	314	100.0

Hall-Héroult cell**Inert anode cell**

3. Conclusions

The thermal-electrical calculations of the inert anodes and stable cathodes show that there are solutions to retrofit an existing technology that can match the best in class existing technologies while producing oxygen as a by-product. There is no need of one extra volt to operate the cell when taking following features into account:

- Semi-vertical anodes and cathodes;
- Reduced shell size;
- Low anode and cathode voltage drops;
- Low and constant ACD between two solids.

Further optimizations are possible on the busbars side and on the lining side to reduce cell voltage drop and thus specific energy consumption.

The authors would like to thank Prof. Vittorio de Nora† who mostly designed such a cell long ago as the chairman of MOLTECH.

4. References

1. Jomar Thonstad, Ioan Galasiu, Rodica Galasiu, *Inert Anodes for Aluminium Electrolysis*, 1st edition Aluminium-Verlag ISBN 978-3-87017-286-2, 2007, p. 15.
2. Halvor Kvande, Inert electrodes in aluminium electrolysis, *Light Metals* 1999, 369-376.
3. Jomar Thonstad, Pavel Fellner, Geir Martin Haarberg, Ján Híveš, Halvor Kvande, Åsmund Sterten, *Aluminium Electrolysis*, 3rd edition Aluminium-Verlag ISBN 3-87017-155-3, 2001, p. 65.
4. Vittorio de Nora and René von Kaenel, Technical and economical evaluation of the de Nora inert metallic anode in aluminium reduction cells, *Light Metals* 2006, 397-402.
5. Vittorio de Nora, René von Kaenel, Jacques Antille and Laurent Klinger, Modeling of a 25 kA de Nora inert metallic anode test cell, *Light Metals* 2006, 391-396.
6. Thin Nguyen and Vittorio de Nora, de Nora oxygen evolving inert metallic anode, *Light Metals* 2006, 385-390.
7. Asbjørn Solheim, Inert Anodes – the Blind Alley to Environmental Friendliness? *Light Metals* 2018, 1253-1260.